Zinc isotope evidence for paleoenvironmental changes during Cretaceous Oceanic Anoxic Event 2

Article *in* Geology · December 2020

DOI: 10.1130/G48198.1

8 authors, including:

Xi Chen
China University of Geosciences (Beijing)
28 PUBLICATIONS **274** CITATIONS
SEE PROFILE

Brad Sageman
Northwestern University
165 PUBLICATIONS **7,365** CITATIONS
SEE PROFILE

Hanwei Yao
China University of Geosciences (Beijing)
9 PUBLICATIONS **22** CITATIONS
SEE PROFILE

Han Kaibo
China University of Geosciences (Beijing)
5 PUBLICATIONS **0** CITATIONS
SEE PROFILE

GEOLOGY | THE GEOLOGICAL SOCIETY OF AMERICA®

https://doi.org/10.1130/G48198.1

Manuscript received 27 July 2020
Revised manuscript received 3 October 2020
Manuscript accepted 6 October 2020

Zinc isotope evidence for paleoenvironmental changes during Cretaceous Oceanic Anoxic Event 2

Xi Chen[1,2]*, Bradley B. Sageman[3], Hanwei Yao[4], Sheng'Ao Liu[2], Kaibo Han[4], Yi Zou[4] and Chengshan Wang[1,4]
[1]State Key Laboratory of Biogeology and Environmental Geology, China University of Geosciences, Beijing 100083, China
[2]Institute of Earth Sciences, China University of Geosciences, Beijing 100083, China
[3]Department of Earth and Planetary Sciences, Northwestern University, Evanston, Illinois 60208, USA
[4]School of Earth Sciences and Resources, China University of Geosciences, Beijing 100083, China

ABSTRACT

Paleoclimate during the Cenomanian-Turonian Oceanic Anoxic Event 2 (OAE 2, 94.5–93.9 Ma) was characterized by elevated atmospheric CO_2 concentrations and peak global temperatures. In this study, we employ $\delta^{66}Zn$ measured on samples spanning OAE 2 in an expanded hemipelagic section in Tibet to trace changes in the major fluxes that influence biogeochemical cycles. The prominent feature of the $\delta^{66}Zn$ record in the studied section is a continuous decrease from ~1‰ at the onset of OAE 2 to a minimum of ~0.2‰ within the Plenus Cold Event (ca. 94.3 Ma), followed by a stepwise recovery through the upper part of OAE 2. The negative shift in $\delta^{66}Zn$ corresponds with higher terrigenous inputs, as revealed by previously published detrital index and TOC/TN (total organic carbon to total nitrogen) ratio records, and covaries with a notable decreasing trend recorded in compiled pCO_2 data of different basins. We propose that influx of isotopically light Zn from weathered volcanic rocks associated with submarine large igneous provinces and/or (sub)tropic Indian continental volcanics is likely responsible for the $\delta^{66}Zn$ decrease. We infer that the recovery of $\delta^{66}Zn$ was caused by continued high primary production and an inevitable decline in the flux of light Zn as volcanic terrains were progressively weathered. The ultimate cessation of OAE 2 may have been a consequence of the same effect, with the nutrient supply from weathering reaching a minimum threshold to maintain productivity-anoxia feedback.

INTRODUCTION

Evidence from numerous studies indicates that Oceanic Anoxic Event 2 (OAE 2, 94.5–93.9 Ma: Jones et al., 2020), spanning the Cenomanian-Turonian boundary, was marked by high atmospheric CO_2 concentrations (pCO_2), rapid global warming, and mass extinction of benthic fauna (e.g., Jenkyns et al., 2017). It is also characterized by widespread marine anoxia and euxinia, which are associated with a positive carbon isotope excursion spanning <1 m.y. (Meyers et al., 2012). In early studies of OAE 2, it was suggested that a dramatic drawdown of pCO_2 may have occurred shortly following the onset of the event due to massive burial of marine organic carbon (Arthur et al., 1988), as evidenced by proxies for pCO_2, e.g., $\delta^{13}C$ values of S-bound phytane and C35 hopane (Sinninghe Damsté et al., 2008), leaf stomatal index (Barclay et al., 2010), and the offset between $\delta^{13}C$ of carbonate and that of organic carbon ($\Delta^{13}C$; Jarvis et al., 2011). The discovery of a positive shift in $\delta^{18}O$ combined with the appearance of cool-water (Boreal) taxa led to definition of the Plenus Cold Event (PCE, ca. 94.3 Ma; Gale and Christensen, 1996; Jones et al., 2020), providing support for this hypothesis, although climate was warming prior to the onset of OAE 2 and continued to warm after the PCE to a peak in the early Turonian (e.g., O'Brien et al., 2017; Gale et al., 2019).

Sequestration of CO_2 to drive a transient cooling event could be forced by both silicate weathering and photosynthetic fixation of carbon into sedimentary organic matter. For the first half of OAE 2, two pulses of increased $\delta^{13}C$ values are globally recorded, which are possibly linked with enhanced productivity and burial of organic carbon (Jarvis et al., 2011). These pulses co-occur with pCO_2 drawdown (e.g., Barclay et al., 2010), suggesting that photosynthetic fixation of carbon is the primary mechanism of CO_2 sequestration. On the other hand, multiple types of isotope data, such as Sr (Frijia and Parente, 2008), Ca (Blättler et al., 2011), and Li (Pogge von Strandmann et al., 2013), have been interpreted to reflect enhanced silicate weathering at this time.

Recently, high-resolution $\delta^{66}Zn$ variations have been studied in sections located around the proto–North Atlantic region (Fig. 1) to investigate zinc cycling and related paleoceanographic changes during the OAE 2 interval (Sweere et al., 2018, 2020). An increase in $\delta^{66}Zn$ values of 0.2‰–0.3‰ during the main phase of the OAE 2 carbon isotope excursion (CIE) is recorded in the organic-rich sediments in the Tarfaya basin (southern Morocco; Sweere et al., 2020) and attributed to extensive burial of isotopically lighter Zn in organic-rich marine sediments globally. Low $\delta^{66}Zn$ values during the PCE were interpreted to result from remobilization of isotopically light Zn from continental-margin sediments owing to reoxygenation of benthic environments (Sweere et al., 2018, 2020). In this study, we present $\delta^{66}Zn$ from an expanded Cenomanian-Turonian section in southern Tibet (Li et al., 2006), which was located at the northern margin of the Indian continent in the eastern Tethys Ocean (Fig. 1), to further investigate the drivers of paleoenvironmental changes during OAE 2.

MATERIALS AND METHODS

We present data for the Cenomanian-Turonian transition interval of the Gongzha section (GPS: 28°42′50.5″N, 86°42′56.7″E) in southern Tibet. Twenty-two (22) samples were collected from section heights of 27 to 66 m to measure Zn isotope ratios. Samples were chosen from the bulk samples used by Zhang et al. (2019) to analyze for $\delta^{13}C_{carb}$ (carb—carbonate) and $\delta^{15}N$.

*E-mail: xichen@cugb.edu.cn

CITATION: Chen, X., et al., 2020, Zinc isotope evidence for paleoenvironmental changes during Cretaceous Oceanic Anoxic Event 2: Geology, v. 49, p. , https://doi.org/10.1130/G48198.1

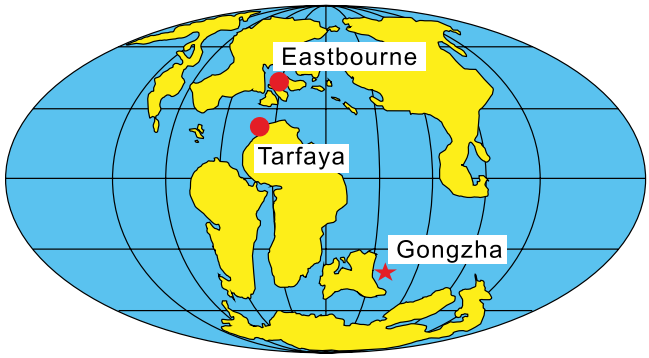

Figure 1. Locations of the Gongzha section (southern Tibet), Eastbourne section (southern UK), and Tarfaya basin (southern Morocco). Paleogeographic reconstruction shows the distribution of land (yellow) and sea (blue) at 100 Ma (after Hay, 2009).

The mean sedimentation rate of the OAE 2 interval in this section is ~40 mm/k.y. (Li et al., 2017). Thus, the studied interval spans ~1 m.y. and the sampling resolution is ~45 k.y., which is ~4× the present-day oceanic residence time of Zn (~11 k.y.; Little et al., 2014).

Our measurement of Zn isotope values strictly followed the method of Liu et al. (2017). Zinc isotopic data are reported in standard δ notation as per mil relative to standard reference material JMC 3-0749L (Maréchal et al., 1999). The whole-procedural reproducibility of Zn isotope analysis of standards and carbonate rocks is better than ±0.10‰ (2σ). Further analytical details for the Zn isotope values, major and trace element concentrations of bulk samples, and trace element concentrations of the carbonate fraction are provided in the Supplemental Material[1].

Li et al. (2017) divided the $\delta^{13}C_{carb}$ curve across OAE 2 into six segments and labeled them C1 to C6 to help facilitate correlation to other OAE 2 sections. Our study largely follows the scheme of Li et al. (2017) except for a slightly different interpretation of the onset for the OAE 2 CIE. According to the definition of O'Connor et al. (2020), the interval from the minor negative trough in $\delta^{13}C$ at ~42 m to the end of segment C3 (~48 m) is equivalent to the PCE. Detailed division of the segments are presented in the Supplemental Material.

[1]Supplemental Material. Sampled section details, analytical methods, and supporting data. Please visit https://doi.org/10.1130/GEOL.S.13232360 to access the supplemental material, and contact editing@geosociety.org with any questions.

RESULTS

For the Gongzha data set, $\delta^{66}Zn$ values average 0.76‰ ± 0.58‰ (2σ; $n = 22$) (Fig. 2). The most notable characteristic of the $\delta^{66}Zn$ curve is the progressive decrease by ~0.8‰ that initiates at the onset of the OAE 2 CIE interval and ends at ~45.1 m (Fig. 2). Below this interval, background $\delta^{66}Zn$ values average 1.02‰ ± 0.20‰ (2σ), which is very similar to that of modern surface seawater (~0.9‰; Little et al., 2014). Values remain low, between 0.2‰ to 0.4‰, in the lower third of segment C4, above which $\delta^{66}Zn$ values increase to 0.9‰ through the upper half and remainder of the CIE interval.

The Zn content of the carbonate fraction is expressed as the Zn/Ca ratio. The Zn/Ca ratio

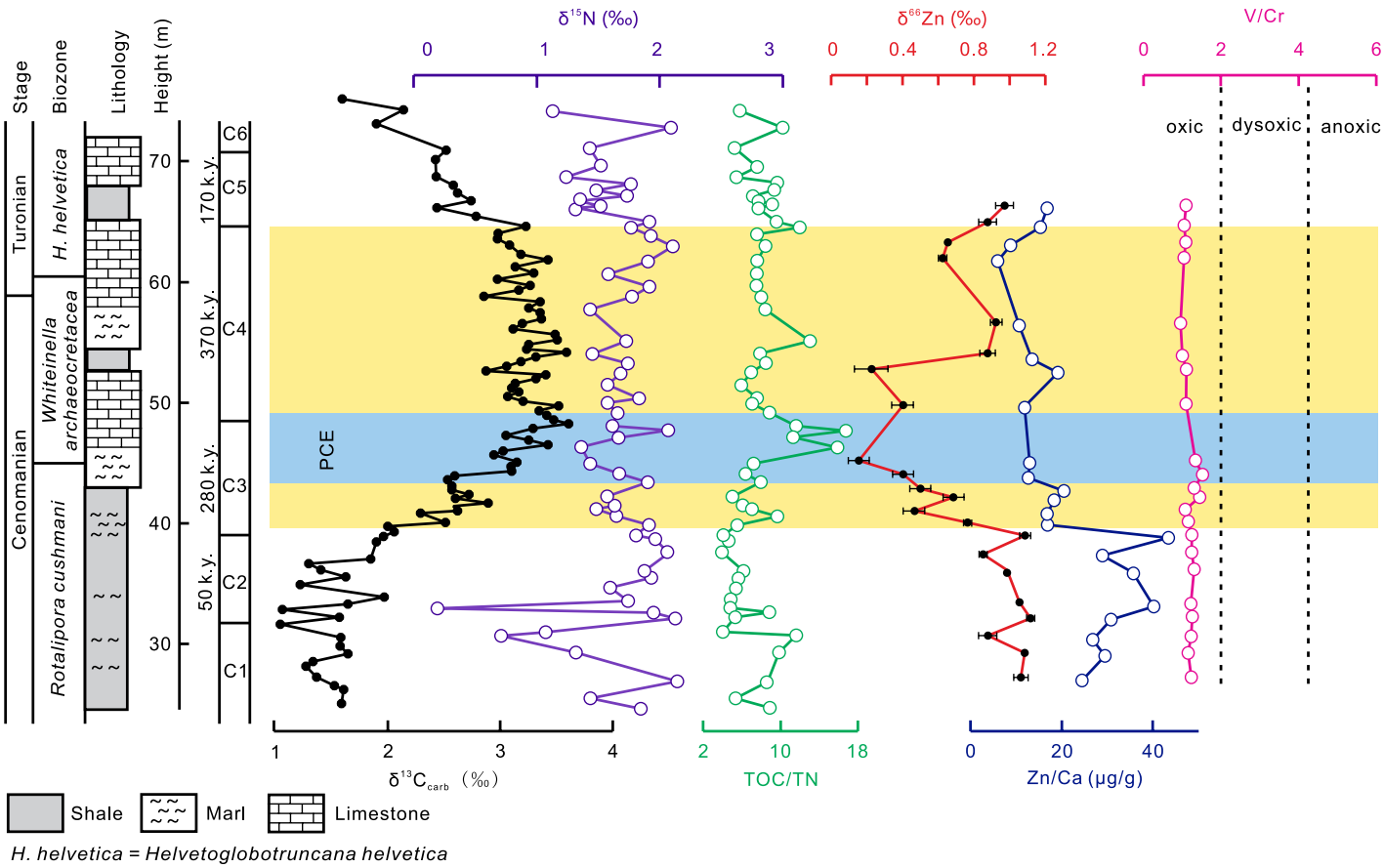

Figure 2. Carbon isotope, $\delta^{15}N$, TOC/TN (total organic carbon to total nitrogen ratio), $\delta^{66}Zn$, Zn/Ca, and V/Cr (bulk sample) plots across Oceanic Anoxic Event 2 (OAE 2) of the Gongzha section in southern Tibet. Segments C1 to C6 and their durations are based on Li et al. (2017). $\delta^{13}C_{carb}$ (carb—carbonate), $\delta^{15}N$, and TOC/TN plots are from Zhang et al. (2019). Division of redox conditions by V/Cr ratio is based on Jones and Manning (1994). Error bars on the $\delta^{66}Zn$ plot represent 2σ. Yellow box and blue band show the OAE 2 and Plenus Cold Event (PCE) intervals respectively.

has an average value of 20.93 ± 20.40 µg/g (2σ) for the studied interval. The background Zn/Ca value averages 32.42 ± 13.17 µg/g (2σ), which is followed by a sharp negative shift to values of ~16 µg/g at the onset of CIE (~40 m section height). Upward, Zn/Ca ratios remain low and continuously decrease to ~6 µg/g at the top of the CIE interval.

We studied minor elements of bulk samples to analyze redox conditions. V/Cr values range from 0.95 to 1.54, indicating oxic bottom waters, which is consistent with previous studies (Bomou et al., 2013). From 42 to 45 m, the V/Cr ratio is slightly enriched (1.31–1.54) but still below the value associated with a transition to dysoxic conditions (Jones and Manning, 1994).

DISCUSSION

Data Evaluation and Reliability

The following evidence indicates that the measured δ^{66}Zn values record a primary seawater signature. First, the δ^{66}Zn values are not associated with changes in precipitation rate or diagenesis, as indicated by the Sr/Ca (Fig. S2 in the Supplemental Material) and δ^{18}O data (Fig. S3). Second, the δ^{66}Zn values do not covary with concentrations of major oxides in bulk sample (e.g., SiO_2 and Al_2O_3; Figs. S4 and S5), indicating that the δ^{66}Zn shift did not result from adsorption of Zn onto silicate or clay minerals. Third, Zn/Mn ratios in the leachates are not associated with changes in δ^{66}Zn (Fig. S6), which indicates that leaching of ferromanganese coatings is not responsible for the δ^{66}Zn variations.

Gongzha Zinc Isotope Record and Comparison to Eastbourne, UK

The δ^{66}Zn curve from Gongzha has some distinctive characteristics compared to the chalk record of the Eastbourne section in the southern United Kingdom (Sweere et al., 2018) (Fig. 3). In the Eastbourne section, a marked negative shift in δ^{66}Zn at the base of the CIE appears to be synchronous with the onset of the negative δ^{66}Zn excursion from Tibet. However, the Eastbourne record shows a significant broad positive excursion before falling to values near 0.5‰ (Sweere et al., 2018).

These different observations are consistent with the suggestion by Sweere et al. (2018) that δ^{66}Zn is likely to show regional variations. Although Sweere et al. (2018) interpreted the main driver of the upper negative shift in δ^{66}Zn as remobilization of isotopically light Zn from organic-rich substrates due to the PCE reoxygenation of bottom waters, this is unlikely to be the major reason for the decrease of δ^{66}Zn values in the lower part of the OAE 2 interval at Gongzha, where the initiation of the negative excursion occurs significantly earlier than the PCE and conditions were oxic through the entire interval. Additionally, magmatism or remobilization of Zn from black shales would lead to transient shifts (Liu et al., 2017; Sweere et al., 2018), but the deceasing trend in δ^{66}Zn at the Gongzha site spans ~175 k.y. Moreover, δ^{15}N values are positive, ranging mainly between 1‰ and 2‰, and lack any secular trend during OAE 2 (Zhang et al., 2019), unlike those of the proto-Atlantic basin that reflect disruptions of the N cycle related to upwelling of nutrient-rich waters and eutrophic conditions (e.g., Kuypers et al., 2004). These results are consistent with Gongzha V/Cr ratios, which indicate consistently oxic conditions.

The similarity of the Tibetan δ^{66}Zn data spanning OAE 2 to trends in δ^{7}Li (depleted values in the first ~200 k.y. of the event; Pogge von Strandmann et al., 2013) suggests an alternate explanation: enhanced weathering of fresh basalts adding isotopically depleted elements to the marine inventory.

Magmatism or reoxygenation of sediments, interpreted previously for the Permian-Triassic boundary (Liu et al., 2017) and in other OAE 2 studies (Sweere et al., 2018), could lead to rapid increases in Zn/Ca ratios. However, the

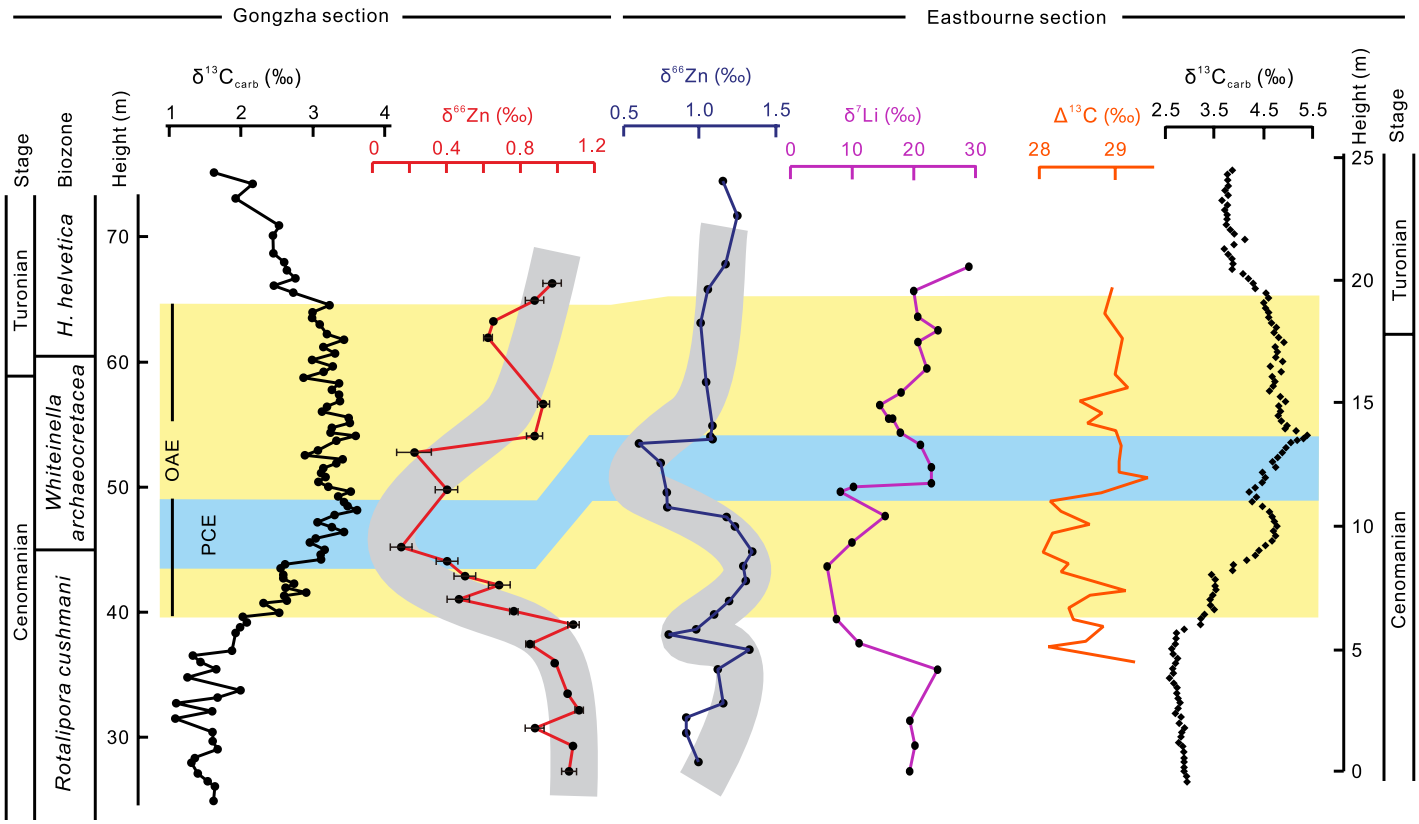

Figure 3. Comparison of δ^{66}Zn and $\delta^{13}C_{carb}$ (carb—carbonate) plots from the Gongzha section (southern Tibet) and Eastbourne section (southern UK) (Sweere et al., 2018). Error bars on the δ^{66}Zn plot represent 2σ. Yellow box area and blue band show Oceanic Anoxic Event 2 (OAE 2) and Plenus Cold Event (PCE) intervals, respectively. Bold gray curves show trends of δ^{66}Zn plots. δ^{7}Li (Pogge von Strandmann et al., 2013) and Δ^{13}C (Jarvis et al., 2011) plots from Eastbourne are also presented. *H. helvetica—Helvetoglobotruncana helvetica*.

temporal variation of Zn/Ca ratios at Gongzha differs from that of prior examples. Although there is a pulse in Zn/Ca just prior to the onset of OAE 2, values rapidly decrease at the onset of CIE segment C3 and remain low throughout the remainder of OAE 2. Significant increase in productivity during the initial part of OAE 2 (CIE segments C2 to C3) is consistent with phosphorus accumulation rate data (Bomou et al., 2013), and it is possible that excess Zn was scavenged by the elevated organic matter flux. Data compiled from literature indicate high pCO_2 at the onset of OAE 2 (O'Connor et al., 2020, and references therein), which would have enhanced weathering rates of both submarine and subaerial basalts. The reason that the δ^{66}Zn record in the proto-Atlantic region does not follow the same trend as the record at Gongzha may be that the Zn cycle in the proto-Atlantic was overcome during the initial stages of OAE 2 by the effect of massive organic-matter burial, which some researchers have argued was dominantly focused in the Atlantic (e.g., Owens et al., 2018). Although δ^{66}Zn initially shifted toward heavier values, the reoxygenation of organic-enriched substrates during the PCE may have ultimately helped to drive δ^{66}Zn mass balance toward more negative values. One final factor that may support this interpretation is the recent discovery of subaerial volcanic deposits of the Caribbean large igneous province (LIP) by Buchs et al. (2018), which suggests that the LIP itself may have reduced water mass exchange between the Pacific and proto-Atlantic basins (as proposed by Trabucho Alexandre et al. [2010]). This hypothesis is consistent with the benthic environment in the Gongzha region being relatively oxic for most of its depositional history, and its δ^{66}Zn record showing no evidence of distinct changes related to the PCE.

Considering processes closer to the study site, high pCO_2 may have also stimulated weathering of the Indian continent. A flux of isotopically lighter Zn from terrestrial sources following the onset of OAE 2 would have driven decreases in δ^{66}Zn values of the eastern Tethys Ocean. Peaks in the TOC/TN (total organic carbon to total nitrogen) ratio (Fig. 2; Zhang et al., 2019) and the detrital influx (Bomou et al., 2013) between 40–48 m could indicate enhanced terrigenous input and thus support this explanation. Lower Cretaceous mafic rocks, which are particularly susceptible to weathering, are widely distributed along the northern margin of the Indian continent (e.g., Zhu et al., 2009). Abundant zircons of Early Cretaceous age (ca. 125 Ma) in Lower Cretaceous volcaniclastic sandstones of the Tethyan Himalaya indicate massive volcanic activity on the Indian continent during that time (e.g., Hu et al., 2010).

Our study allows for the possibility that weathering on land may have contributed to changes in the marine Zn inventory. During the Late Cretaceous, the northern margin of the Indian continent was located at ~30°S (Huang et al., 2015). Given a much lower latitudinal temperature gradient than the present day, the climate of this region could have been (sub)tropical. Enhanced weathering intensity under such conditions could have significantly influenced pCO_2 drawdown, especially given the "supergreenhouse" conditions of the late Cenomanian–early Turonian (Kent and Muttoni, 2013). The weathering of continental basalts in modern warm climate zones, such as Southeast Asia and India, consumes CO_2 at a rate of $\sim 1.6 \times 10^{12}$ mol/yr and is the most important sink for atmospheric CO_2 (Dessert et al., 2003). We suggest that the weathering of Cretaceous mafic rocks widely developed on the Indian continent and elsewhere may have contributed to the substantial pCO_2 drawdown during deposition of the lower half of segment C3.

In segments C4 and C5, δ^{66}Zn shows a stepwise recovery to pre-OAE values. Although the increase in pCO_2 (e.g., O'Connor et al., 2020) could have led to lighter Zn inputs from continental weathering, the positive shift in δ^{66}Zn suggests that primary production persisted, and this is supported by continued enriched values of δ^{13}C. Eventually δ^{13}C values reach a new baseline, marking the end of OAE 2. This may simply reflect a progressive decrease in the nutrient flux from weathering (i.e., Robinson et al., 2019) such that a minimum threshold to maintain productivity-anoxia feedback in the global ocean was achieved.

SUMMARY

This study presents a new δ^{66}Zn data set for OAE 2 in an expanded section from southern Tibet. Zinc isotope values in the Gongzha section reflect mainly an enhanced flux of isotopically light Zn from intensified weathering of volcanic rocks; these could be related to the Caribbean LIP, older volcanic terrains on the Indian continent, or both. The Gongzha data set provides a useful comparison to the Eastbourne δ^{66}Zn record, resulting in a hypothesis of possible basin restriction and massive organic-carbon burial in the proto-Atlantic region. Depleted δ^{66}Zn values in the Gongzha section characterize the PCE, and remobilization of lighter Zn from organic facies may have played a role, but Gongzha facies are pervasively oxic without significant changes in redox condition and the negative trend in δ^{66}Zn begins well before the PCE. Our data more strongly support a hypothesis of elevated chemical weathering intensity resulting in massive but short-term sequestration of carbon following the onset of OAE 2. The long-term return of δ^{66}Zn to background values likely reflects a high uptake by organisms and an inevitable decline in the flux of light Zn from exposed volcanics.

ACKNOWLEDGMENTS

This work was financially supported by the National Natural Science Foundation of China (grants 41888101 and 41672104). We are grateful to comments from H. Jenkyns, S. Batenburg, and one anonymous reviewer. Sageman thanks the Fulbright Commission for funding support during the writing of this paper.

REFERENCES CITED

Arthur, M.A., Dean, W.E., and Pratt, L.M., 1988, Geochemical and climatic effects of increased marine organic-carbon burial at the Cenomanian/Turonian boundary: Nature, v. 335, p. 714–717, https://doi.org/10.1038/335714a0.

Barclay, R.S., McElwain, J.C., and Sageman, B.B., 2010, Carbon sequestration activated by a volcanic CO_2 pulse during Ocean Anoxic Event 2: Nature Geoscience, v. 3, p. 205–208, https://doi.org/10.1038/ngeo757.

Blättler, C.L., Jenkyns, H.C., Reynard, L.M., and Henderson, G.M., 2011, Significant increases in global weathering during Oceanic Anoxic Events 1a and 2 indicated by calcium isotopes: Earth and Planetary Science Letters, v. 309, p. 77–88, https://doi.org/10.1016/j.epsl.2011.06.029.

Bomou, B., Adatte, T., Tantawy, A.A., Mort, H., Fleitmann, D., Huang, Y., and Föllmi, K.B., 2013, The expression of the Cenomanian–Turonian oceanic anoxic event in Tibet: Palaeogeography, Palaeoclimatology, Palaeoecology, v. 369, p. 466–481, https://doi.org/10.1016/j.palaeo.2012.11.011.

Buchs, D.M., Kerr, A.C., Brims, J.C., Zapata-Villada, J.P., Correa-Restrepo, T., and Rodríguez, G., 2018, Evidence for subaerial development of the Caribbean oceanic plateau in the Late Cretaceous and palaeo-environmental implications: Earth and Planetary Science Letters, v. 499, p. 62–73, https://doi.org/10.1016/j.epsl.2018.07.020.

Dessert, C., Dupré, B., Gaillardet, J., François, L.M., and Allègre, C.J., 2003, Basalt weathering laws and the impact of basalt weathering on the global carbon cycle: Chemical Geology, v. 202, p. 257–273, https://doi.org/10.1016/j.chemgeo.2002.10.001.

Frijia, G., and Parente, M., 2008, Strontium isotope stratigraphy in the upper Cenomanian shallow-water carbonates of the southern Apennines: Short-term perturbations of $^{87}Sr/^{86}Sr$ during the Oceanic Anoxic Event 2: Palaeogeography, Palaeoclimatology, Palaeoecology, v. 261, p. 15–29, https://doi.org/10.1016/j.palaeo.2008.01.003.

Gale, A.S., and Christensen, W.G., 1996, Occurrence of the belemnite *Actinocamax plenus* in the Cenomanian of SE France and its significance: Bulletin of the Geological Society of Denmark, v. 43, p. 68–77.

Gale, A.S., et al., 2019, High-resolution bio- and chemostratigraphy of an expanded record of Oceanic Anoxic Event 2 (Late Cenomanian–Early Turonian) at Clot Chevalier, near Barrême, SE France (Vocontian Basin): Newsletters on Stratigraphy, v. 52, p. 97–129, https://doi.org/10.1127/nos/2018/0445.

Hay, W.W., 2009, Cretaceous oceans and ocean modeling, *in* Xiumian, H., et al., eds., Cretaceous Oceanic Red Beds: Stratigraphy, Composition, Origins, and Paleoceanographic and Paleoclimatic Significance: SEPM (Society for Sedimentary Geology) Special Publication 91, p. 243–271.

Hu, X., Jansa, L., Chen, L., Griffin, W.L., O'Reilly, S.Y., and Wang, J., 2010, Provenance of Lower Cretaceous Wölong Volcaniclastics in the Tibetan Tethyan Himalaya: Implications for the

final breakup of eastern Gondwana: Sedimentary Geology, v. 223, p. 193–205, https://doi.org/10.1016/j.sedgeo.2009.11.008.

Huang, W., van Hinsbergen, D.J.J., Lippert, P.C., Guo, Z., and Dupont-Nivet, G., 2015, Paleomagnetic tests of tectonic reconstructions of the India-Asia collision zone: Geophysical Research Letters, v. 42, p. 2642–2649, https://doi.org/10.1002/2015GL063749.

Jarvis, I., Lignum, J.S., Gröcke, D.R., Jenkyns, H.C., and Pearce, M.A., 2011, Black shale deposition, atmospheric CO_2 drawdown, and cooling during the Cenomanian-Turonian Oceanic Anoxic Event: Paleoceanography, v. 26, PA3201, https://doi.org/10.1029/2010PA002081.

Jenkyns, H.C., Dickson, A.J., Ruhl, M., and van den Boorn, S.H.J.M., 2017, Basalt-seawater interaction, the Plenus Cold Event, enhanced weathering and geochemical change: Deconstructing Oceanic Anoxic Event 2 (Cenomanian–Turonian, Late Cretaceous): Sedimentology, v. 64, p. 16–43, https://doi.org/10.1111/sed.12305.

Jones, B., and Manning, D.A.C., 1994, Comparison of geochemical indices used for the interpretation of paleo-redox conditions in ancient mudstones: Chemical Geology, v. 111, p. 111–129, https://doi.org/10.1016/0009-2541(94)90085-X.

Jones, M.M., Sageman, B.B., Selby, D., Jicha, B.R., Singer, B.S., and Titus, A.L., 2020, Regional chronostratigraphic synthesis of the Cenomanian-Turonian Oceanic Anoxic Event 2 (OAE2) interval, Western Interior Basin (USA): New Re-Os chemostratigraphy and $^{40}Ar/^{39}Ar$ geochronology: Geological Society of America Bulletin, https://doi.org/10.1130/B35594.1.

Kent, D.V., and Muttoni, G., 2013, Modulation of Late Cretaceous and Cenozoic climate by variable drawdown of atmospheric pCO_2 from weathering of basaltic provinces on continents drifting through the equatorial humid belt: Climate of the Past, v. 9, p. 525–546, https://doi.org/10.5194/cp-9-525-2013.

Kuypers, M.M.M., van Breugel, Y., Schouten, S., Erba, E., and Sinninghe Damsté, J.S., 2004, N_2-fixing cyanobacteria supplied nutrient N for Cretaceous oceanic anoxic events: Geology, v. 32, p. 853–856, https://doi.org/10.1130/G20458.1.

Li, X., Jenkyns, H.C., Wang, C., Hu, X., Chen, X., Wei, Y., Huang, Y., and Cui, J., 2006, Upper Cretaceous carbon- and oxygen-isotope stratigraphy of hemipelagic carbonate facies from southern Tibet. China: Journal of the Geological Society, v. 163, p. 375–382, https://doi.org/10.1144/0016-764905-046.

Li, Y., Montañez, I.P., Liu, Z., and Ma, L., 2017, Astronomical constraints on global carbon-cycle perturbation during Oceanic Anoxic Event 2 (OAE2): Earth and Planetary Science Letters, v. 462, p. 35–46, https://doi.org/10.1016/j.epsl.2017.01.007.

Little, S.H., Vance, D., Walker-Brown, C., and Landing, W.M., 2014, The oceanic mass balance of copper and zinc isotopes, investigated by analysis of their inputs, and outputs to ferromanganese oxide sediments: Geochimica et Cosmochimica Acta, v. 125, p. 673–693, https://doi.org/10.1016/j.gca.2013.07.046.

Liu, S., Wu, H., Shen, S., Jiang, G., Zhang, S., Lv, Y., Zhang, H., and Li, S., 2017, Zinc isotope evidence for intensive magmatism immediately before the end-Permian mass extinction: Geology, v. 45, p. 343–346, https://doi.org/10.1130/G38644.1.

Maréchal, C.N., Télouk, P., and Albarède, F., 1999, Precise analysis of copper and zinc isotopic compositions by plasma-source mass spectrometry: Chemical Geology, v. 156, p. 251–273, https://doi.org/10.1016/S0009-2541(98)00191-0.

Meyers, S.R., Siewert, S.E., Singer, B.S., Sageman, B.B., Condon, D.J., Obradovich, J.D., Jicha, B.R., and Sawyer, D.A., 2012, Intercalibration of radioisotopic and astrochronologic time scales for the Cenomanian-Turonian boundary interval, Western Interior Basin, USA: Geology, v. 40, p. 7–10, https://doi.org/10.1130/G32261.1.

O'Brien, C.L., et al., 2017, Cretaceous sea-surface temperature evolution: Constraints from TEX_{86} and planktonic foraminiferal oxygen isotopes: Earth-Science Reviews, v. 172, p. 224–247, https://doi.org/10.1016/j.earscirev.2017.07.012.

O'Connor, L.K., Jenkyns, H.C., Robinson, S.A., Remmelzwaal, S.R.C., Batenburg, S.J., Parkinson, I.J., and Gale, A.S., 2020, A re-evaluation of the Plenus Cold Event, and the links between CO_2, temperature, and seawater chemistry during OAE 2: Paleoceanography and Paleoclimatology, v. 35, e2019PA003631, https://doi.org/10.1029/2019PA003631.

Owens, J.D., Lyons, T.W., and Lowery, C.M., 2018, Quantifying the missing sink for global organic carbon burial during a Cretaceous oceanic anoxic event: Earth and Planetary Science Letters, v. 499, p. 83–94, https://doi.org/10.1016/j.epsl.2018.07.021.

Pogge von Strandmann, P.A.E., Jenkyns, H.C., and Woodfine, R.G., 2013, Lithium isotope evidence for enhanced weathering during Oceanic Anoxic Event 2: Nature Geoscience, v. 6, p. 668–672, https://doi.org/10.1038/ngeo1875.

Robinson, S.A., Dickson, A.J., Pain, A., Jenkyns, H.C., O'Brien, C.L., Farnsworth, A., and Lunt, D.J., 2019, Southern Hemisphere sea-surface temperatures during the Cenomanian–Turonian: Implications for the termination of Oceanic Anoxic Event 2: Geology, v. 47, p. 131–134, https://doi.org/10.1130/G45842.1.

Sinninghe Damsté, J.S., Kuypers, M.M.M., Pancost, R.D., and Schouten, S., 2008, The carbon isotopic response of algae, (cyano)bacteria, archaea and higher plants to the late Cenomanian perturbation of the global carbon cycle: Insights from biomarkers in black shales from the Cape Verde Basin (DSDP Site 367): Organic Geochemistry, v. 39, p. 1703–1718, https://doi.org/10.1016/j.orggeochem.2008.01.012.

Sweere, T.C., Dickson, A.J., Jenkyns, H.C., Porcelli, D., Elrick, M., van den Boorn, S.H.J.M., and Henderson, G.M., 2018, Isotopic evidence for changes in the zinc cycle during Oceanic Anoxic Event 2 (Late Cretaceous): Geology, v. 46, p. 463–466, https://doi.org/10.1130/G40226.1.

Sweere, T.C., Dickson, A.J., Jenkyns, H.C., Porcelli, D., and Henderson, G.M., 2020, Zinc- and cadmium-isotope evidence for redox-driven perturbations to global micronutrient cycles during Oceanic Anoxic 2 (Late Cretaceous): Earth and Planetary Science Letters, v. 546, 116427, https://doi.org/10.1016/j.epsl.2020.116427.

Trabucho Alexandre, J., Tuenter, E., Henstra, G.A., van der Zwan, K.J., van de Wal, R.S.W., Dijkstra, H.A., and de Boer, P.L., 2010, The mid-Cretaceous North Atlantic nutrient trap: Black shales and OAEs: Paleoceanography, v. 25, PA4201, https://doi.org/10.1029/2010PA001925.

Zhang, X., Gao, Y., Chen, X., Hu, D., Li, M., Wang, C., and Shen, Y., 2019, Nitrogen isotopic composition of sediments from the eastern Tethys during Oceanic Anoxic Event 2: Palaeogeography, Palaeoclimatology, Palaeoecology, v. 515, p. 123–133, https://doi.org/10.1016/j.palaeo.2018.03.013.

Zhu, D., Chung, S., Mo, X., Zhao, Z., Niu, Y., Song, B., and Yang, Y., 2009, The 132 Ma Comei-Bunbury large igneous province: Remnants identified in present-day southeastern Tibet and southwestern Australia: Geology, v. 37, p. 583–586, https://doi.org/10.1130/G30001A.1.

Printed in USA